AFRL-SR-AR-TR-04-

0612

REPORT DOCUMENTATION PAGE

1. REPORT DATE *(DD-MM-YYYY)*	2. REPORT TYPE	3. DATES COVERED *(From - To)*
21-09-2004	Final Report	6/1/01 - 11/30/03

4. TITLE AND SUBTITLE
Light weight and Flexible Organic Memory cells for Satellite Application

5a. CONTRACT NUMBER

5b. GRANT NUMBER
F49620-01-1-0427

5c. PROGRAM ELEMENT NUMBER

6. AUTHOR(S)
Prof. Yang Yang

5d. PROJECT NUMBER

5e. TASK NUMBER

5f. WORK UNIT NUMBER

7. PERFORMING ORGANIZATION NAME(S) AND ADDRESS(ES)
AND ADDRESS(ES) The Regents of the University of California
Department of Materials Science and Engineering
University of California, Los Angeles
6531 Boelter Hall
Los Angeles, CA 90095
Tel: 310-825-4052
Fax: 310-825-3665

8. PERFORMING ORGANIZATION REPORT NUMBER

9. SPONSORING / MONITORING AGENCY NAME(S) AND ADDRESS(ES)
USAF, AF Office of Scientific Research
4015 Wilson Blvd., Room 713
Arlington, VA 22203-1954

NL

10. SPONSOR/MONITOR'S ACRONYM(S)

11. SPONSOR/MONITOR'S REPORT NUMBER(S)

12. DISTRIBUTION / AVAILABILITY STATEMENT
Distribute to the public.

13. SUPPLEMENTARY NOTES
The views, opinions and/or findings contained in this report are those of the author(s) and should not be constructed as an official U.S. Air Force position, policy or decision, unless so designated by other documentation.

14. ABSTRACT

This Final Report to the AFOSR provides an account of the summary progress that have been achieved on organic bistable device (OBD), with primary focus being on the theoretical modeling and experimental characterization we established for the OBD project and its possibility usage in space satellites. The most spectacular recent achievement has been the successful understanding of the underlying mechanism and improving of the device performance. Another achievement involves the selection of a novel class of material used in OBD for satellite application. Finally, we have tested organic material for the space application, and the initial results showed that organics are more durable than most people thought, perhaps due to its amorphous structure.

We have met that objective in the past with a minimal number of personnel and equipment by relying on our theoretical might and experimental technique to provide a "force multiplication" advantage. We have applied the theoretical model to improve the OBD performance. The modified OBD was then subjected to extensive experimental characterization. The results in turn confirmed the validity of using the model. Last, but not least, we have collaborated with JPL to test the organic materials and devices under high energy x-ray radiation. The preliminary data suggests that the organic compounds used in OBD are good candidates for space application.

15. SUBJECT TERMS

16. SECURITY CLASSIFICATION OF:			17. LIMITATION OF ABSTRACT	18. NUMBER OF PAGES	19a. NAME OF RESPONSIBLE PERSON
a. REPORT	b. ABSTRACT	c. THIS PAGE	Unlimited		Yang Yang
					19b. TELEPHONE NUMBER *(include area code)* (310) 825-4052

Standard Form 298 (Rev. 8-98)
Prescribed by ANSI Std. Z39.18

DISTRIBUTION STATEMENT A
Approved for Public Release
Distribution Unlimited

Final Technical Report to AFOSR

Project title: Light Weight and Flexible Organic Memory Cells for Satellite Application

Grant Number: F49620-01-1-0427

Program Director: Dr. Charles Lee

PI: Prof. Yang Yang
Department of Materials Science and Engineering
UCLA
6531 Boelter Hall
Los Angeles, CA 90095

Date: September 21, 2004

Achievements

This Final Report to the AFOSR provides an account of the summary progress that have been achieved on organic bistable device (OBD), with primary focus being on the theoretical modeling and experimental characterization we established for the OBD project and its possibility usage in space satellites. The most spectacular recent achievement has been the successful understanding of the underlying mechanism and improving of the device performance. Another achievement involves the selection of a novel class of material used in OBD for satellite application. Finally, we have tested organic material for the space application, and the initial results showed that organics are more durable than most people thought, perhaps due to its amorphous structure.

We have met that objective in the past with a minimal number of personnel and equipment by relying on our theoretical might and experimental technique to provide a "force multiplication" advantage. We have applied the theoretical model to improve the OBD performance. The modified OBD was then subjected to extensive experimental characterization. The results in turn confirmed the validity of using the model. Last, but not least, we have collaborated with JPL to test the organic materials and devices under high energy x-ray radiation. The preliminary data suggests that the organic compounds used in OBD are good candidates for space application.

Status of the research

To summarize briefly the characteristics of our OBD, we first start by reviewing a multilayer structure of electrode/organic/metal/organic/electrode; it shows a very unique electrical bistability and non-volatile memory behaviors, indicating that once the device

is switched to a high conductivity state, it remains on that state even the external voltage is removed. The transition time from the low conductance state to the high conductance state is of a nano-second scale. To switch the device back to the low conductivity state, it requires simply a negative bias. Following this successful demonstration of the feasibility of our OBD for practical use, we created a mathematical model to explain its underlying operation mechanism. With the better understanding of the physics behind, we tried to enhance the device performance by selecting proper materials and designing better device structure. Lastly, the organic compounds were subjected to x-ray radiation test, and the results indicated that ability of the compounds to survive in space was promising.

This Annual Report is organized as follows; we first present the mathematical calculation which includes the very details explanation of all the parameters governing the device electrical properties. Then the possible materials to enhance and stabilize the OBD performance are suggested. The experimental characterization of the core element – nano-particle middle layer of the OBD is shown and discussed. A model based on our mathematical calculation and experimental observation is then presented. Lastly, the radiation test on the organic materials and devices and it implications for space application is present and discussed.

Mathematical Calculation

Based on the former experimental results on Organic Bistable Device (OBD), we have tried to create a model for OBD based on theoretical calculation so as to understand the operating mechanism better. The middle layer of our memory device is very critical

to the device performance; it is suggested to be a mixture of nano-particles with organic molecules. We believe that the mechanism of the bistable phenomenon is caused by the charge transferred from one facet of the organic layer to the other, forming a unique kind of electrical charge trapping phenomenon in the nano-particle layers. The calculation of transmission probability helps use to conclude that the charges in the nano-particle layer take a very important role in fixing the transport properties of the device. The following model provides a clear explanation on the observed phenomena of the electrical bistbility and the nonvolatile memory effect.

(I). Introduction of the model

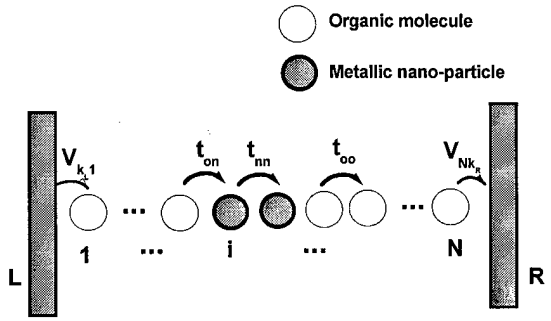

Fig. 1. The schematic diagram of the structure of ODB for calculation. L and R mean the left and right electrodes. t_{on}, t_{nn} and t_{oo} are the hopping terms explained in the text. V_{K_L1} and V_{NK_R} are the interactions between the electrodes and the organic molecules.

We consider a one-dimensional system including two electrodes, organic molecules, and metallic nano-particles (Fig.1). According to recently experiment results, the metallic nano-particles were represented as metal nano-particle cores coated with organic molecules or oxides. This is important in our theory, because as one can see below, the charges stored in the nano-particles are the origin of the bistable memory. The Hamiltonian of the system can be written as

$$H = H_0 + V$$

where H_0 is the Hamiltonian for the noninteracting parts (left, right electrodes, the organic molecules and the metallic nano-particles), and V is the interaction between the electrodes and the organic molecules. The noninteracting Hamiltonian H_0 includes

$$H_0 = H_E + H_{MN}$$

here

$$H_E = \sum_{P \in L,R} \sum_{k_P \sigma} \varepsilon_{k_P \sigma} a^+_{k_P \sigma} a_{k_P \sigma}$$

is the Hamiltonian of the left and right electrodes. $a^+{}_{k_P,\sigma}(a_{k_P,\sigma})$ is the creation (annihilation) operator for an electron with spin σ and energy $\varepsilon_{k_p,\sigma}$, k is the wave vector. We will use the Newns's chemisorption theory to deal with the effect of electrodes on the organic molecules with the metallic nano-particles.

$$H_{MN} = \sum_{i,j,\sigma} (t_{ij} - t_0(i)\delta_{ij}) c^+_{i\sigma} c_{j\sigma} + \frac{1}{2} \sum_{i\sigma} U(i) n_{i\sigma} n_{i-\sigma}$$

is the Hamiltonian of the organic molecules with the metallic nano-particles. $c^+{}_{i\sigma}(c_{i\sigma})$ is the creation (annihilation) operator for an electron with spin σ at the site i for the organic molecules or the metallic nano-particles. $n_{i\sigma} = c^+{}_{i\sigma} c_{i\sigma}$ is the number operator with spin σ at site i. $U(i)$ are the Coulomb interactions for the organic molecules and the metallic nano-particles at site i. t_{ij} are the hopping terms between the electrons at nearest neighbor sites. t_{0i} is the on-site Coulomb interaction at site i. The Hubbard model is used to represent the organic molecules and the metallic nano-particles. Here each site represents an organic molecule or a nano-particle. The thickness of the organic molecules are represented by the numbers of the left and right sites of the left and right molecules (d_{01} and d_{02}). The total thickness of the device is represented by the total number of the

sites $N = d_{01} + d_{02} + d_n$. At large $U(i)$ limit, the electronic energy band is split into two subbands --"up" subband and "low" subband -- which separated by a energy gap of $U(i)$.

$$V = \sum_{P \in R,L} \sum_{k_P,i,\sigma} V_{k_P i} a^{+}_{k_P,\sigma} c_{i,\sigma} + h.c.$$

is the interaction between the organic molecules and the electrodes. $V_{K_P i}(P = L, R)$ is the strength of the interaction between electrodes and the nearest molecules. We assume that the left electrode can only interact with the nearest molecule, while the right electrode interacts with the last molecule.

(II). Calculation of electrical current

We consider the transport of electrons through the organic molecules with the metallic nano-particles by modeling it as a one-electron elastic scattering problem. An electron incident from the left electrode with energy E, has a transmission probability $T(E)$ to scatter into the right electrode. In the system, we suppose that the coupling between the two electrodes is weak, then we can use the Landauer formula to calculate the transmitted current as a function of the bias voltage, Φ,

$$I = \frac{e}{\pi\hbar} \int_0^{\infty} [F(E) - f(E + e\Phi)] T(E) dE,$$

where $f(E)$ is the Fermi distribution. The energy difference in the Fermi function of the left and right electrodes comes from the applied bias voltage Φ. At zero temperature and in the limit $\Phi \to 0$

$$I = \frac{e^2}{\pi\hbar} T(E_F)\Phi$$

here E_F is the Fermi level of the system. This means that the transmission probability near the Fermi level is most important for the electric current at zero temperature.

The transmission probability can be obtained from the scatting theory

$$T(E) = 4\pi^2 \sum_{k_L k_P} | T_{k_L k_R} |^2 \ \delta(E - E_L)\delta(E - E_R) .$$

Where $T_{k_L k_R} = \langle k_L | T | k_R \rangle$ is the transmission amplitude from a state k_L in the left electrode to a state k_R in the right electrode with energy E. $E_L(E_R)$ is the energy of electrons in the left (right) electrode. T is an operator in the scattering theory. In the weak coupling limit of the two electrodes, the T operator

$$T = V + VGV .$$

is usually replaced by its second term only. The first "direct" term V vanishes because there is no direct interaction between the states of the left and right electrodes. $G(E) = (E - H + i0^+)^{-1}$ is the Green function of the system. Thus we get

$$T(E) = 4\pi^2 \, | G_{1N}(E) |^2 \ \Gamma_L(E)\Gamma_R(E) ,$$

where $G_{1N}(E)$ is the (1,N) element of the Green function of the system in a matrix representation. $\Gamma_P(E)(P \in L, R)$ is

$$\Gamma_P(E) = \sum_{k_P} V_{k_P i}{}^2 \delta(E - E_P)$$

The summation is over all the eigenstates of the left (right) electrode.

(III). Solution to the Green function

The basic quantity to be calculated is the retarded single-electron Green function *G(E)*, which includes all relevant information about system. In the matrix representation with a basis including the two electrodes, the organic molecules and the metallic nano-particles, the Green function is the inverse of an infinite matrix. The Hamiltonian matrix is also an infinite matrix. Mujica et. al. have proved that the Hamiltonian matrix can be exactly mapped into a reduced matrix defined in the space of states of the molecular wire, hence of dimension $N \times N$. In our system, the infinite matrix of the Hamiltonian can be mapped into a $N \times N$ matrix of the organic molecules with the metallic nano-particles

subspace. Let H_{MN} be the matrix of the Hamiltonian of the organic molecules with the metallic nano-particles, then the reduced Hamiltonian matrix of the system, $\overline{H}_{MN}$, differs from H_{MN} only in both the first and last diagonal elements, (1,1) and (N,N), which are explicitly given by

$$(\overline{H}_{MN})_{11} = (H_{MN})_{11} - \Pi_1(E),$$
$$(\overline{H}_{MN})_{NN} = (H_{MN})_{NN} - \Pi_N(E)$$

where $\Pi_{1(N)}(E)$ is a self-energy contribution of the electrodes given by

$$\Pi_1(\mathrm{E}) = \sum_{\mathrm{k_L}} \frac{V_{k_L 1}^2}{E - E_L + i0^+} = \Lambda_L(E) - i\Delta_L(E)$$

In the Newns chemisorption theory, $\Lambda_L(E)$ and $\Delta_L(E)$ have the forms

$$\Lambda_L(E) = \begin{cases} \frac{V_{k_L 1}^2}{\gamma_2^2} E, & \left|\frac{E}{\gamma}\right| < 1 \\ \frac{V_{k_L 1}^2}{\gamma_2^2}(E + \sqrt{E^2 - \gamma^2}), & \left|\frac{E}{\gamma}\right| < -1 \\ \frac{V_{k_L 1}^2}{\gamma_2^2}(E - \sqrt{E^2 - \gamma^2}), & \frac{E}{\gamma} > 1 \end{cases}$$

and

$$\Delta_L(E) = \begin{cases} \frac{2V_{k_L 1}^2}{\gamma_2^2}(E + \sqrt{\gamma^2 - E^2}), & \left|\frac{E}{\gamma}\right| < 1 \\ 0, \quad otherwise \end{cases}$$

where γ is half the electrodes energy bandwidth, and E is measured from the center of the energy band of the electrodes. The similar expression for $\Pi_R(E)$ can be obtained.

After the partition technique solution, the problem of the Green function is reduced to solve the Green function of the organic molecules and the metallic nano-particles with additional self-energy terms of electrodes to the (1,1) and (N,N) elements. Thus we only need to solve Green function of the Hubbard model. However, the Hubbard model is a nontrivial problem, it can be solved only in some special cases. In the paper, we use spectral density approach to the Hubbard model, which leads to a rather

convincing result of the Hubbard model. In the following, we give only a brief derivation of the SDA solution and refer the reader to previous papers for a detailed discussion.

At present, the Green function becomes

$$G(E)=\begin{pmatrix} \varepsilon_{1\sigma}(E) & t_{12} & 0 & \vdots & 0 \\ t_{21} & \varepsilon_{2\sigma}(E) & t_{23} & & \vdots \\ 0 & & \ddots & & \\ \vdots & & & \varepsilon_{N-1\sigma}(E) & t_{N-1,N} \\ 0 & \cdots & 0 & t_{N,N-1} & \varepsilon_{N\sigma}(E) \end{pmatrix}^{-1},$$

here $\varepsilon_{i\sigma}(E)=E-t_{0i}-\Sigma_{i\sigma}(E)+\Pi_i(E)\delta_{i1}+\Pi_i(E)\delta_{iN}$. $\Sigma_{i\sigma}(E)$ is the site-dependent electronic self-energy which incorporates all the effects of the electron correlations.

The key point of the SDA is to find a reasonable ansatz for the self-energy. Guided by the precise solvable atomic limit of vanishing hopping (t_{ij}=0) and by the findings of Harris and Lange in the strong-coupling limit (U(i)/t_{ij}>>1), a one-pole ansatz for the self-energy $\Sigma_{i\sigma}(E)$ can be motivated:

$$\Sigma_{i\sigma}(E)=U(i)n_{i-\sigma}\frac{E-B_{i-\sigma}}{E-B_{i-\sigma}-U(i)(1-n_{i-\sigma})}$$

The self-energy depends on the spin-dependent occupation numbers $n_{i\sigma}$ and the so-called band-shift $B_{i\sigma}$. The band occupation can be obtained from the imaginary part of the Green function

$$n_{i\sigma}=-\frac{1}{\pi}\int_{-\infty}^{+\infty}dEf(E)\,\mathrm{Im}G_{ii\sigma}(E)$$

The band-shift $B_{i\sigma}$ consists of higher correlation functions:

$$B_{i\sigma}=t_{0i}+\frac{1}{n_{i\sigma}(1-n_{i\sigma})}\sum_{i\neq j}t_{ij}\left\langle c_{i\sigma}^{+}c_{j\sigma}(2n_{i-\sigma}-1)\right\rangle$$

Although $B_{i\sigma}$ consists of higher correlation functions, it can be expressed exactly via Im $G_{i\sigma}$ and $\Sigma_{i\sigma}(E)$:

$$B_{i\sigma}=t_{0i}-\frac{1}{n_{i\sigma}(1-n_{i\sigma})}\frac{1}{\pi\hbar}\int_{-\infty}^{+\infty}dEf(E)$$

$$\times(\frac{2}{U(i)}\sum_{i\sigma}(E)-1)[E-E_{i\sigma}(E)-t_{0i}]\mathrm{Im}\,G_{i\sigma}(E)$$

Now a closed set of equations for the Green function is established via the above equations, which can be solved self-consistently.

(V). Results and discussions

In our calculations, we keep the Coulomb interaction in the organic molecules fixed at U_o = 2.0eV. The Coulomb interaction in the metallic nano-particles fixed at U_n = 0.5eV. The bandwidths of the two electrodes are 2γ = 10.0eV. The center of the energy band in the left electrode is located at the Fermi level (E_F), while in the right electrode is above the Fermi level by a energy of $e\Phi$ due to the applied electrical bias Φ. The Fermi level is set to zero. The hopping terms between the organic molecules, between the metallic nano-particles, and between a molecule and a nano-particle are set to be smaller than that used in the literature for the conductance in molecular wires. Because the hopping term represents the overlapping between the nearest electrons, the electron hops intermolecularly in our system, while it happens intramolecular in the molecular wires. It is showed that the conductance of molecular wires through the molecular overlapping is two orders smaller than through one molecule. This means the hopping terms between nearest molecules are about one order smaller than between nearest atoms within a molecule. In the following, the hopping term between the nearest organic molecules is defined is too, the term between the nearest organic molecules and the metallic nano-particle as ton, and the term between the nearest nano-particles is t_{nn}. We will refer to the considered structure electrode/organic molecules/nano-particles/organic molecules/ electrode as d_{o1}/ d_n/ d_{o2}, where d_{o1} = d_n= d_{o2} are the thicknesses of the left and right organic molecular layers, dn is the thickness of the metallic nano-particles.

Notice that the spatial profile of the electrostatic potential is not considered in our calculation. This profile will affect the local energy terms t_{0i}. On the other hand, the change of local energy terms will affect the distribution of the spatial concentration of the electrons. These effects should be solved simultaneous the coupling quantum mechanic equation and Poisson equation. In our calculation, we fixed the number population for each site, and adjust the local energy term to fit the band occupation. In addition, we assume that the electrical neutral state is the state where each site has a band occupation of $n_i = 1.0$. Thus the charged state refers to the state with $n_i \neq 1.0$ for any site. For the noncharged states, the number population of each site is $n_i = 1.0$, the local energy for the organic molecules is set t_0 = -1.0eV, and that for the nano-particles is t_0 = -0.25eV. The charged state is a metastable state, it cannot be obtained from the self-consistent solution of the Hamiltonian. There are two ways to get the charged states: first one is fixing the Fermi energy for the whole system, and adjust the local energy for each site to fit the number population of each site. This corresponds to adjusting the electrostatic potential of each site. The second one is fixing the local energy and adjusts the Fermi energy for each site. The possible reason for the charged state in the experiment is that when the applied bias is applied, the electrostatic potential for the device will have a distribution from left electrode to the right electrode. When the difference of electrostatic potential between nearest neighbor nano-particles equals to the gap of the energy level of nano-particles, the electrons will tunnel resonantly from one nano-particle to the nearest neighbor nano-particle. However, we will not deal with the formation of the charged state, rather we will study the difference of the transmission probabilities between charged and without charged states. On the other hand, there may exist many self-

consistent solutions for the Hamiltonian model, here we are only interested in the non-ferromagnetic solution and calculate the self-consistent solution from a higher temperature to a lower temperature.

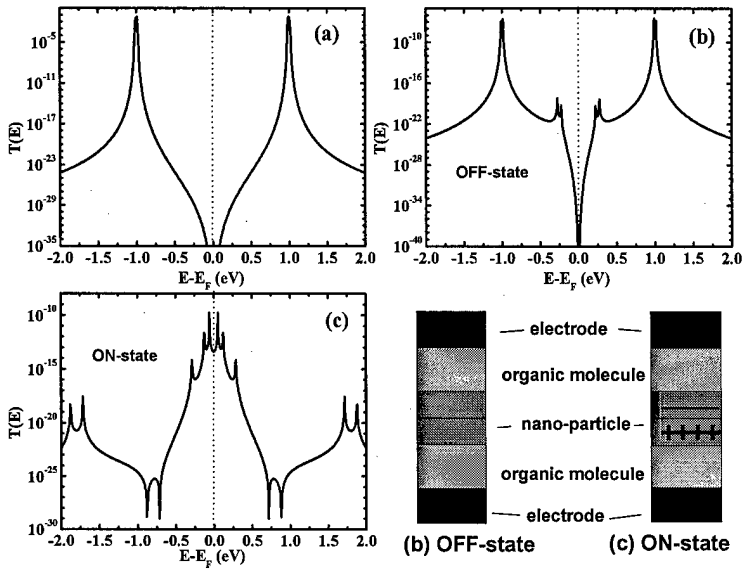

FIG. 2. The transmission probabilities $T(E)$ as a function of energy for the following cases: (a) pure six-layer organic molecular film; (b) 2/2/2 structure and without electrons charged in nano-particles ($n(3)$ = $n(4)$ = 1.0); (c) 2/2/2 structure with electrons charged in the nano-particle layer ($n(3)$ = 1.4; $n(3)$ = 0.6). The schematic structures of the device for the OFF-state and ON-state are plotted at the right corner. Other parameters are: t_{oo} = t_{on} = 0.025eV, t_{nn} = 0.05eV, Φ = 0.0V, T = 50K, V_{K_L1} = V_{NK_R} = 0.05eV, the band occupation of organic molecules are no = 1.0

First, let us see the influence of the metallic nano-particles on the properties of the organic molecular films. In figure 2, we plot the transmission probabilities as a function of energy for the cases with and without the nano-particles. Without the nano-particles (Fig.2a), the transmission probability renders several peaks at the energy around $E = \pm 1.0\,\mathrm{eV}$. Because the Coulomb repulsion between the organic molecules is Uo=2.0 eV, the molecules energy band locates around $E = \pm 1.0\,\mathrm{eV}$. This means an electron with this energy will tunnels resonantly through the organic molecules. For other energy regime, $T(E)$ is very small. When a thin metallic nano-particle layer is added to the

organic molecular films (Fig.2b and 2c), the transmission probabilities change significantly, especially for the case with electrons charged in the metallic nano-particles (Fig.2c). For the case where the metallic nano-particle is not charged (Fig.2b), two small additional peaks of $T(E)$ appears at the energies around $E = \pm 0.25$ eV, which are where the energies of the metallic nano-particle energy band locates. Because the Fermi level is located at the gap between the two Hubbard subbands of the organic molecules and of the metallic nano-particles, the transmission probability is very small at the Fermi level. This means the conductance of the system is very small for the case without the metallic nano-particle layer, and the case with the metallic nano-particles but without charges trapped in it. However, when the electrons are charged in the metallic nano-particles (Fig.2c), the situation changes significantly. As one can see from Fig.2c, the charges in the metallic nano-particles take an important role to the transmission probability, especially at the energy near the Fermi level. At the charged case, $T(E)$ at the Fermi level becomes much higher than the case without charged. $T(E)$ also exists some peaks at the energies around the Fermi level, which are corresponding to the energy bands of the metallic nano-particles. The peaks of $T(E)$ induced by the organic molecules energy bands shifts to the energies farther from the Fermi energy ($E \sim \pm 1.8$ eV) in the charged case compared to the case without charged. In the case charged state (Fig.2c), $T(E)$ is much higher around the Fermi energy than the case without charged. This will induce large electrical current in the structure. As to the I-V behavior of the experiment, when the electric bias is first applied and as the current increases slowly, the metallic nano-particles will have no charges trapped in it. This is corresponding to the OFF-state in Fig.2b. As the applied bias voltage increases, the potential for the electrons in the nano-particles close to the

anode will drop while the potential near the cathode increases. At the switch bias voltage, the electrons at the metallic nano-particles close to the anode will tunnel to the other side, forming the state of different charges trapped in the metallic nano-particles. This will result in the rapid increase of the electric current in the system (from Fig.2b to Fig.2c). When the bias decreases, this state remains due to the barrier between two neighboring nano-particles, so the system remains in a high conductance state (ON-state). With a small negative bias discharging the electrons, the system will be in the state without charges trapped in the metallic nano-particles. This is the low conductance state (Fig.2b). We would like to point out that if the ON-state is a metastable state, the electron should be trapped in the nano-particles. This means that there must exist a potential barrier between the two nano-particles on both sides, so that the electrons can be stored in the nano-particles. This is exactly what the experiment shows. Because in our recently experiments, the memory phenomenon only appears for the case where the middle metallic nano-particles were coated with the organic molecules or oxides.

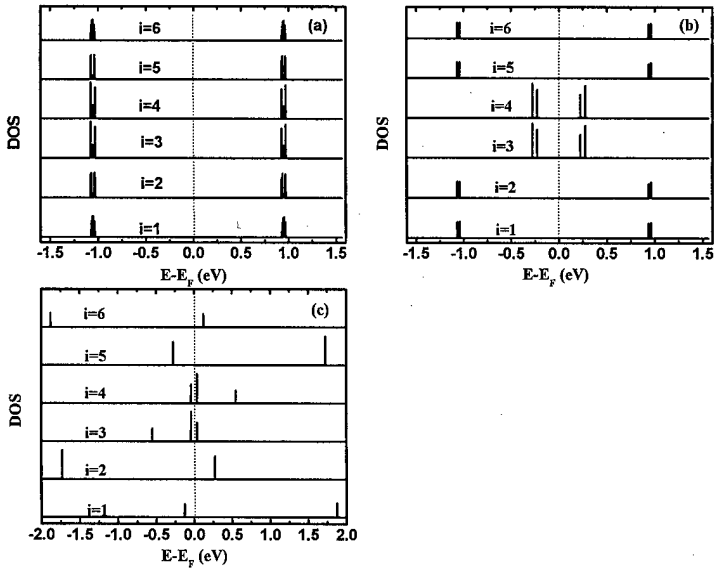

FIG. 3: The layer-dependent density of states as a function of energy for the cases as in Fig.2. All the parameters are same with Fig.2.

The layer-dependent density of states (DOS) is showed in Fig. 3 for the cases as in Fig.2. The strong Coulomb interaction between the electrons causes the spectrum to split into a high and low energy parts ("Hubbard splitting"). These two subbands ("Hubbard bands") are separated by an energy amount of the order $U(i)$. In the one dimensional system, the upper and lower subbands containted several isolated peaks. Without the hopping effect, the peaks will appear only at the energies levels of the upper (corresponding to LUMO) and lower (corresponding to HOMO) Hubbard bands of the organic molecules and the eigenvalues of metallic nano-particles. Due to the hopping effect, each peak splits into several little peaks. In the case of charged state (see Fig.3c), the peaks of the DOS in the metallic nano-particles (i = 3; 4) shift in a different way. The resultant peaks of the DOS in the organic molecules (i = 1; 2; 5; 6) also shift in different ways. Thus there exist several peaks around the Fermi level. This is the reason why $T(E)$ is much higher around Fermi energy in this case.

Now let us turn to the influence of the hopping term on the organic molecules. The hopping dependence of $T(E_F)$ at Fermi level is plotted in Fig. 4. $T(E_F)$ increases quickly as the hopping term $t_{oo} = t_{on}$ increases at small t_{oo}. It will reach a saturation value as t_{oo} increases to a large value. This means that increasing the overlap between the organic molecules will increase the conductance of the organic molecules and the nano-particles system. This is because as the hopping increases, the electrons are easier to transmit through the regime of the organic molecules and the metallic nano-particles.

The effect of the thickness $d_{o1} = d_{o2} = d_o$ of the organic molecules on $T(E_F)$ is plotted in figure 6. As the thickness of the organic molecules increases, the ability to scatter electrons increases too. Thus the transmission probability will decrease. One can

see that $T(E_F)$ decreases exponentially as t_o increases. This is the same as the theoretical results obtained in the pure molecular wires in the case of the small hopping term. This is because the hopping term is much smaller compared to the energy gaps of the molecules.

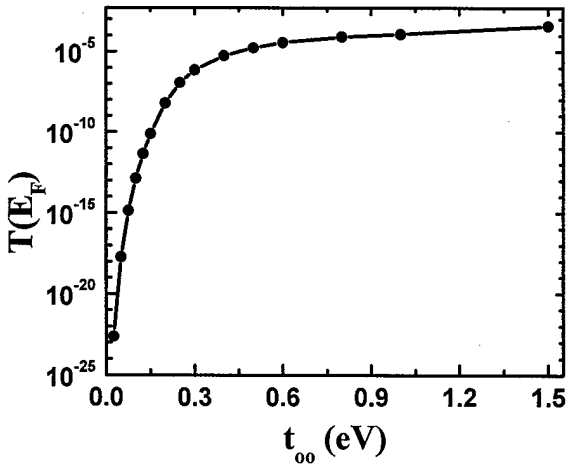

FIG. 4: The transmission probability $T(E_F)$ as a function of the hopping term too between nearest sites in organic molecules in the case of different charges trapped in nano-particles (ON-state). Other parameters are: $t_{oo} = t_{on} = 0.025$eV, $t_{nn} = 0.05$eV, $\Phi = 0.0$V, T = 50K, $V_{K_L 1} = V_{NK_R} = 0.05$eV, T = 50K, no = 1.0, n(3) = 1.4, n(3) = 0.6.

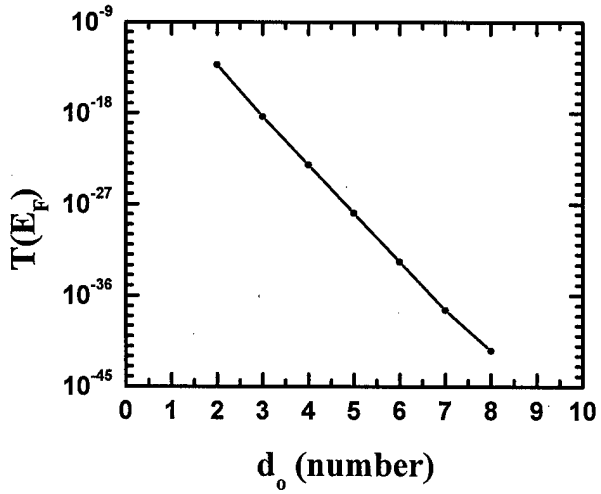

FIG. 5: The transmission probability $T(E_F)$ at the Fermi level as a function of the thicknesses $d_o = d_{o1} = d_{o2}$ of the organic molecules in the case of different electrons charged in the metallic nano-particles (ON-state). Other parameters are same with Fig. 4.

We believe that the mechanism of the bistable phenomenon is caused by the charges transfer from one side to the other forming a different kind of electrical charge trapping in the nano-particle layers. By the calculation of transmission probability, we found that the electrons charged in the nano-particle took a very important role for the transport properties of the ODB. The transmission probabilities of the charged states change significantly compared to the case without charged. The transmission probability decreases exponentially as the thickness of the organic molecules increases. The transmission probability will increase as the hopping term of the organic molecules increases. But the hopping dependence of the transmission probability is neither a linear one nor an exponential one.

Organic material selection

We have observed that the organic materials used for OBDs play a significant role in determining the device performance. Based on the experimental characterization of several organics (including polymers), they can be divided into two categories: relatively high and relatively low conducting materials. The chemical structures are illustrated in Fig. 6. The results suggest that organic materials with high dielectric constants and low conductivity provide better performances.

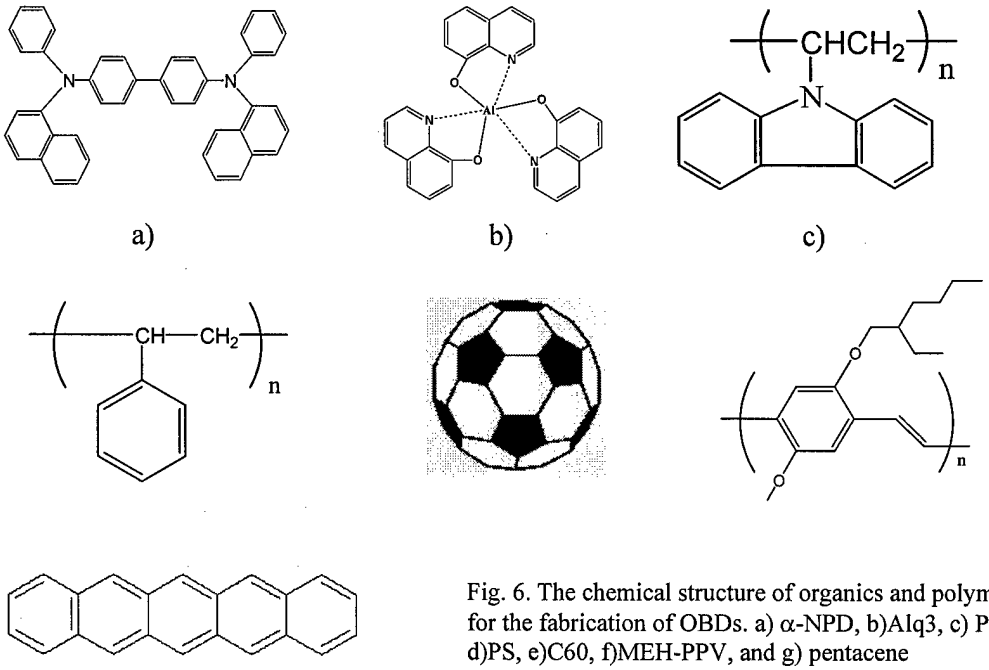

Fig. 6. The chemical structure of organics and polymers for the fabrication of OBDs. a) α-NPD, b)Alq3, c) PVK, d)PS, e)C60, f)MEH-PPV, and g) pentacene

(MEH-PPV, C60 and Pentacene), show similar electrical bistable phenomena. This is shown in Fig. 7. Devices with MEH-PPV, $C_{60,}$ or pentacene, which are high conductivity (or high mobility), no electrical bistable phenomena are observed. The conductivity (or mobility) of the organic compound seems plays an important role of determining the electrical and memory effect.

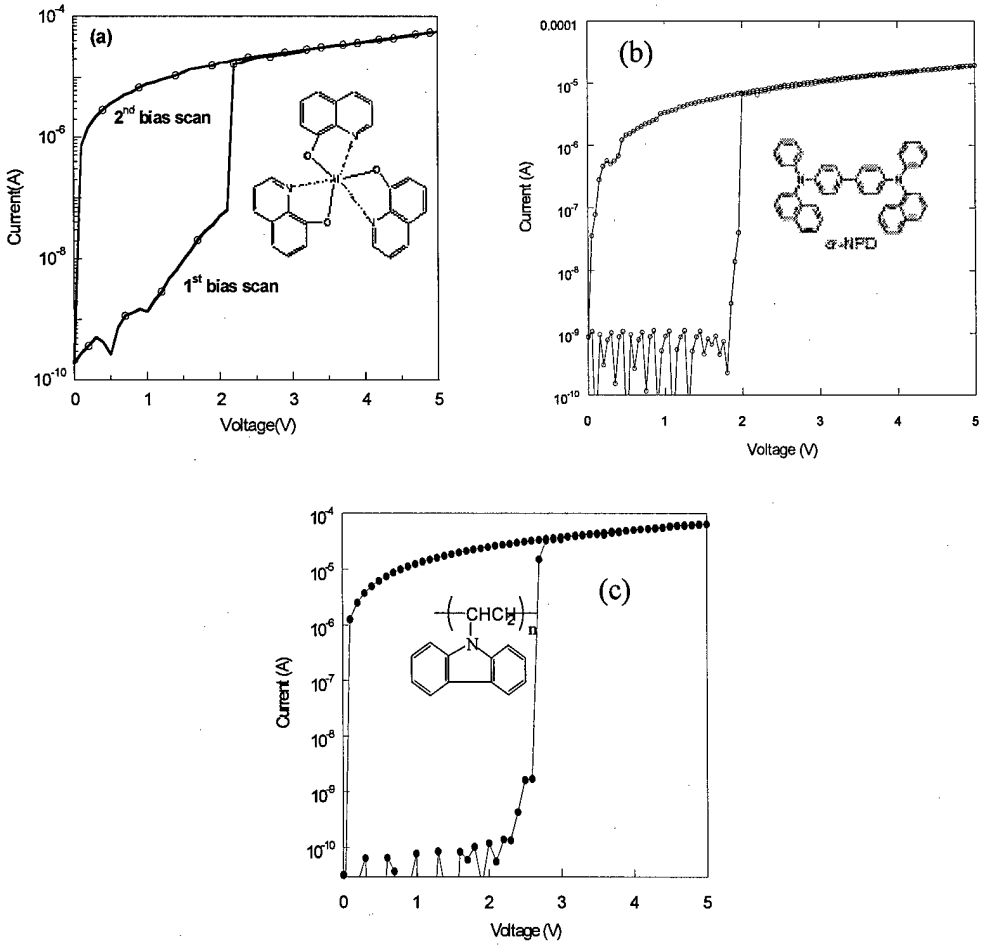

Fig.7. Current-voltage characteristics of OBDs with a) Alq3, b)α-NPD, and c)PVK

The characteristics of middle metal layer

Our previous study illustrated the fact that in order to observe electrical bistability the thickness of the middle metal layer should be larger than the critical thickness, which is around 10 nm. We have realized that two 10 nm-thick middle metal layers, which are prepared with different evaporation rates, 0.3 and 2.0 Å/s respectively, shows different characteristics. Finally, we found that this is a very important parameter to make high performance OBDs.

In order to understand the characteristics of the 10 nm-thick middle metal layer prepared under different evaporation rates, a simple experiment was carried out to *in-situ* measure the conductivity of the middle metal layer during evaporation. The experimental setup and results are shown in Fig. 8.

In case of 0.3 Å/s, the percolation threshold of the Al-nanoclusters occurs at ~8 to 10 nm. This thickness is consistent with the appearance of the electrical bistability phenomena of our OBD device. It is worth noting that the resistance of the 50 nm-thin film is ~1000 ohm, which is far above the resistance of pure metallic Al thin film (less than 0.01 ohm). This observation suggests that the film consists of a mixture of Al metal and metal oxide that is formed during the evaporation of the middle Al layer with the presence of residue oxygen inside the chamber. This experiment suggests that the deposited Al is in fact not pure metallic Al, and the percolation threshold of the Al layer occurs at ~10 nm. It is likely that the Al nanocluster is surrounded by thin oxide layer.

It is worth noting that in the case of relatively high evaporation rate, 2 Å/s, the thickness dependence on the resistance curve has the same shape as that of low

evaporation rate. But, the overall resistance of the film is slight lower at same thickness. The percolation threshold of the Al-nanocluster occurs around 4.5 nm, which is a little smaller than that with 0.3 Å/s. It is worth to emphasize that organic bistability and the memory effect can only be achieved with material evaporated at slow rate. This indicates that the composition of the middle metal layer can be controlled by changing the evaporation rate and the composition, that is, the ratio of metal and metal oxide which play a very important role in making OBDs.

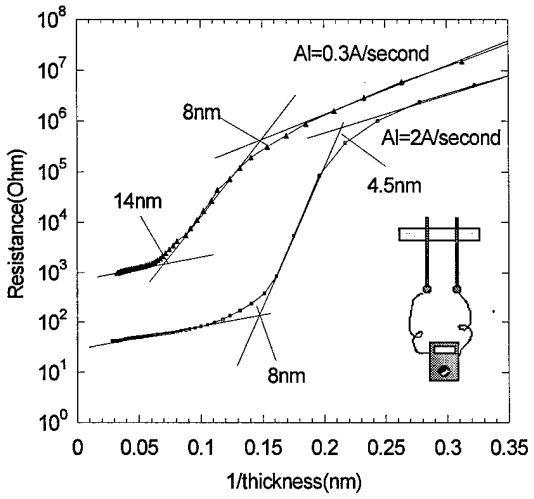

Fig. 8. The experimental illustration and results for the *in-situ* resistance measurement of Al-nanocluster layer on top of the AIDCN film. For comparison, two evaporation rates were used, 0.3 Å/second and 2Å/second. For the case of 0.3 Å/second, the resistance is ~1000 ohms at 50nm thickness, which indicates the film is not pure metal but a mixture of metal and metal oxide

The results suggest that the Al nanocluster is surrounded by thin oxide layer results from the slow evaporation rate of Al. This argument is consistent with the optical transparency of the thin film, as well as the AFM image shown in Fig. 9. Fig. 9 shows a 200 nm square AFM image of the Al-nanocluster layer with 4 nm in thickness. It can be seen from Fig. 4 that the deposited Al layer consists of nanoclusters about 8 nm in diameter covering the surface granular structure of the lower organic layer.

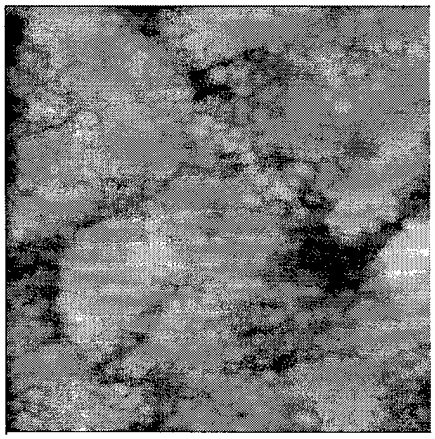

Fig. 9. A 200 nm square AFM images of the 4nm thick Al-nanocluster layer on top of AIDCN/Al with electrode.

In order to further confirm the oxide formation in the middle layer, XPS spectroscopy was performed to measure the core electron energy level of Al. The results are shown in Fig. 10, which indicate the formation of an oxide layer (77.2 eV peak) in a thickness of 8 to 16 Å when Al was deposited onto an AIDCN film. With the thickness of 8 Å, the coexistence of Al and Al-oxide is clearly seen.

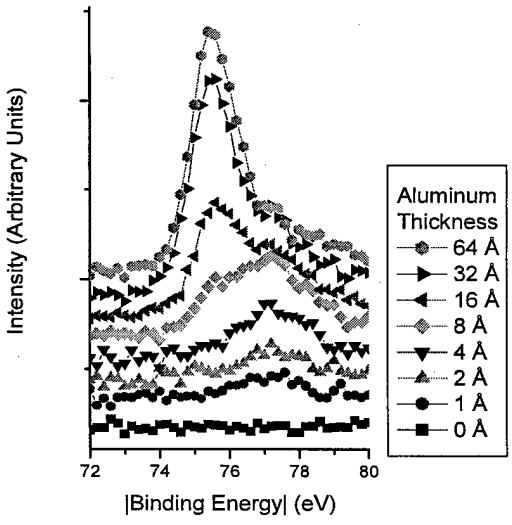

Fig. 10. XPS spectra of Al incrementally deposited on AIDCN as a function of Al thickness. The peak of 77.2 eV for Al-oxide suggests that the initial phase of the Al thin film is in the oxide form. At the thickness of 8Å, the coexistence of Al and Al-oxide is clearly seen.

Understanding the mechanism of OBDs

Based on our understanding of the electrical characteristics of the middle metal layer and the effect of different organics on electrical bistability and the memory effect, we propose an energy model which is shown in Fig.11. The assumption is that each Al-nanocluster has a pure metallic core and an oxide coating. The middle metal layer embedded in the organic layers act as a layer for charge trapping, where the oxide coating creates a charge transport barrier. The energy band diagram of the unbiased Al middle layer shows a distribution of many energy wells next to each other, which are sandwiched between the two organic layers with high LUMO-HOMO energy levels, as shown in Fig. 11(a).

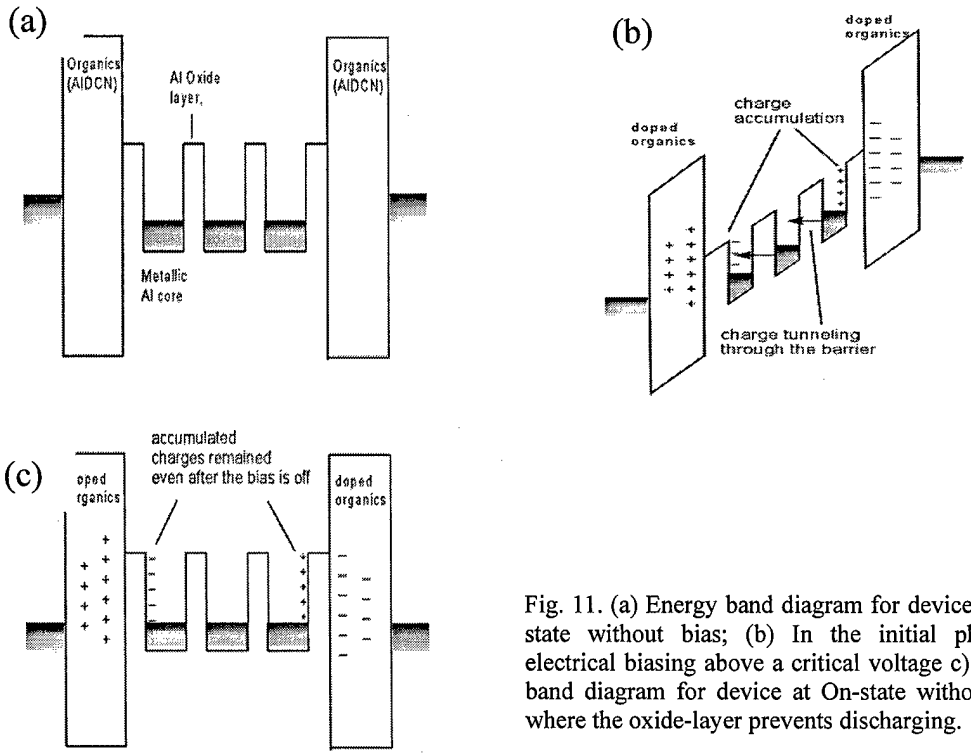

Fig. 11. (a) Energy band diagram for device at Off-state without bias; (b) In the initial phase of electrical biasing above a critical voltage c) Energy band diagram for device at On-state without bias, where the oxide-layer prevents discharging.

Upon bias over a critical value (~2 V), as shown in Fig. 11(b), electrons start to tunnel from one energy well to another against the direction of the applied electric field. Negative charges will be trapped (or stored) on one side of the wells and positive charges will be trapped on the other side of the wells because of the oxide layer and the thick AIDCN layer with relatively high HOMO-LUMO energy levels. The stored charges at both sides of the energy wells subsequently induce charges within the organic layers and significantly reduced the resistance of the organic layers.

Supporting argument for proposed mechanism model with specially designed experiment

To confirm the argument accounts for the memory effect, the conductivity of the organic layer has been measured accordingly. As illustrated in Fig. 12(a), two identical OBDs have been fabricated side-by-side. Electrode A and B are the anodes for these two OBDs, respectively, and electrode C is the common cathode. The I-V curves for OBD-A and OBD-B (Fig 12(b)) are similar to that of typical OBD. The conductivity of the bottom organic layer can be determined through the measurement of current between electrode A and B by applying a very small voltage scan (from 0 to 0.1 V), which will not trigger the electrical bistability. As shown in Fig 11(c), when the voltage is 0.1 V, the current injected to the organic film is different by four orders of magnitude between On-state and Off-state, which is quite consistent with the electrical bistability in the OBD devices.

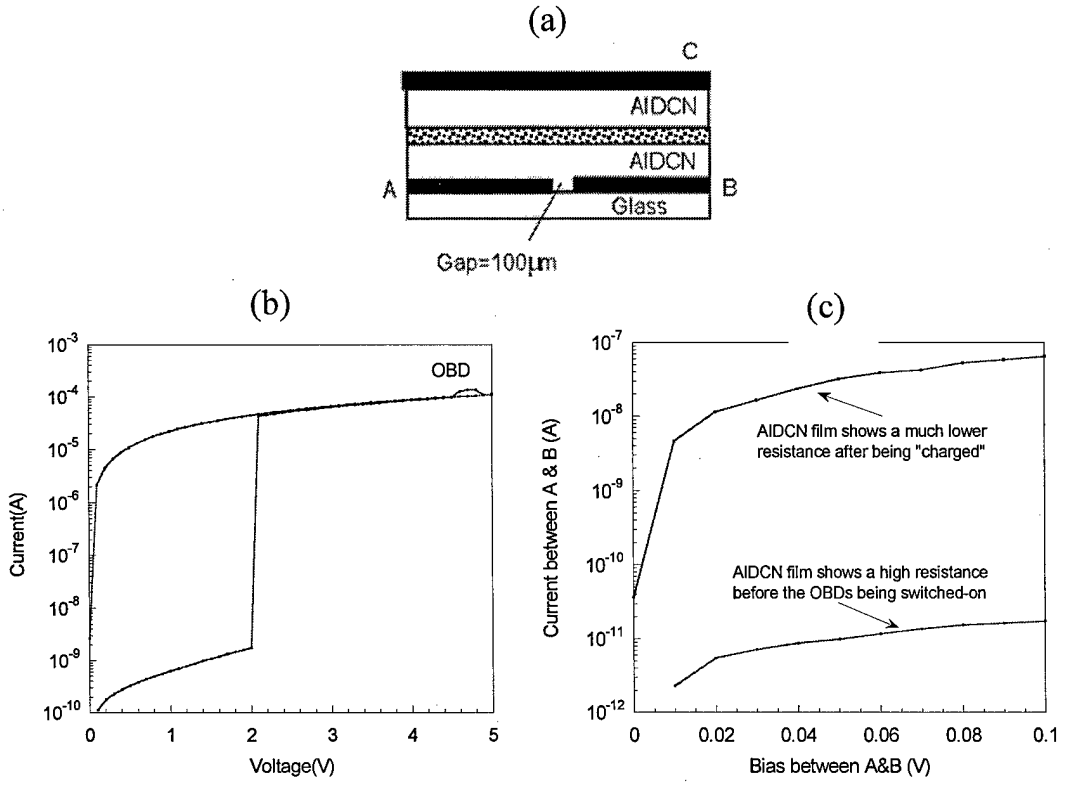

Fig. 11. An experiment designed to measure the resistance of the organic layer in the ON-state and OFF-state. (a) The device structure of two OBDs built side-by-side with anodes A and B and a common cathode C. (b) I-V curves for OBD-A and OBD-B. (c) The current between electrode A and B for the ON-state and OFF-state. The difference of the current is about four orders in magnitude, similar to the difference of electrical bistability in these two devices.

Radiation Test:

A preliminary radiation test on the organic devices has been conducted, in collaboration with JPL and AFR, with primary focus being on their susceptibility to radiation damage. The results are encouraging. In the test, organic TFTs were subjected to X-ray source up to 1M Rad, and showed no sign of degradation. The experiments are still underway at AFRL and we will provide the latest results in few weeks.

Experimental Setup

- Transistor design: Three samples were fabricated and delivered to AFRL
    1) Top contact, pentacene thin film transistors fabricated at JPL
    2) Bottom contact, pentacene thin film transistor fabricated at JPL
    3) Bottom contact, sexithiophene thin film transistor fabricated at UCLA
- X-ray source parameters: Tungsten target, 50 kV accelerating voltage, 10 mA beam current
- Radiation conditions: 30.6 krad/min (Si), ca. 10-60 keV bremsstrahlung
- Instrumentation: HP 4145B under control by ICS Metrics software
- Shielding: A lead sheet approximately 1mm thick with a single hole drilled in it with diameter ca. 5 mm was placed over the sample. The hole allows radiation to strike the sample such that a single 5000 μm x 500 μm transistor is fully irradiated, though portions of adjacent consecutive numbered transistors will be irradiated as well.
- Given the time constraints, and the necessity to identify suitable irradiation ranges and conditions, only a few devices were tested. The details of these devices were:
    - Sample number 1 (top contact pentacene TFTs)
    - Device number: 5000-500-1 through 5000-500-6
    - Device geometry: gate length = 500 μm, gate width = 5000 μm

The preliminary results suggest that when there is no bias to the gate, the device shows no damage to its electrical performance. However, when the gate is biased during the radiation test, device shows a significant amount of leakage current; a possible reason for this observation is the damage of the gate oxide. Further investigations are still underway and we will provide the latest progress to AFOSR.

Summary:

We have made significant progress on the understanding of the underlying mechanism of our OBDs. A model which explains most of the observed OBD electrical phenomena has been proposed and the experimental observation shows the validity of using the mathematical model. Radiation tests on organic TFTs shows that organic compounds are quite robust when exposed to radiation test. However, the silicon oxide layer might be subjected to the radiation damage; this becomes an obstacle for us to continue the test. A better selection of the oxide layer used in device is crucial to the progress of the OBD project.

This project is fruitful and productive. The invention has been transferred to an private company and subsequently acquired by AMD, the second largest semiconductor manufacture in the US.

Our initial results about organic applications in the space has been very helpful and this will be another important area for the organic/polymeric electronics in the next several years.

Personnel Supported

Three students and two post-doc have been supported under this project.

1. **Ms. Yan Saho** and **Mr. Douglas Severs** at the Department of Materials Science and Engineering are responsible for the fabrication of OBD and I-V characterization. **Dr. Qianfei Xu** received her PHD degree with honor from the School of Engineering and Applied Science. She joined Johns Hopkins University as a postdoc fellow from October 2004.
2. This grant also supports two postdocs: Dr. Liping Ma and Dr. Jianyong Ouyang.
3. We also deeply appreciate the technical discussion with Dr. Qibing Pei at Stanford Research Institute and Prof. Fred Wudl at Department of Chemistry and Biochemistry.

Publications

1. Liping Ma, Jie Liu, Seungmoon Pyo, Qianfei Xu, andYang Yang, "Organic bistable devices", Molecular Crystals and Liquid Crystals, 378, 185-192, (**2002**).

2. Liping Ma, Jie Liu, Seungmoon Pyo and Yang Yang, "Organic bistable light-emitting devices", Appl. Phys. Lett., .80, 362, (**2002**).

3. Liping Ma, Jie Liu and Yang Yang, "Organic electrical bistable devices and rewritable memory cells", Appl. Phys. Lett. 80, 2997, (**2002**).

4. Liping Ma, Seungmoon Pyo, Jiangyong Ouyang, Qiangei Xu, and Yang Yang, "Observation from current step to bistability in organic/Al-nanocluster/organic system", Submitted to J. of Appl. Phys.

5. Liping Ma, Seungmoon Pyo, Jianyong Ouyang, Qianfei Xu, and Yang Yang, "Nonvolatile electrical bistability of organic'metal-nanocluster'organic system", Appl. Phys. Lett. **82**, 1419, (**2003**).

6. Jianhua Wu, Liping Ma, and Yang Yang, "Single-band Hubbard model for transport properties in bistable organic/metallic nanoparticle/organic devices", Physical Review B, 69, 115321, **(2004)**

7. Jianyong Ouyang and Yang Yang, "Write-Once-Read-Many Organic Electronic Memory (WORM)", Adv. Materials, submitted, (**2004**).

8. Jun He, Liping Ma, and Yang Yang, "Electric Field Distribution of Organic Bistable Device and a Three-Terminal Organic Memory Devices", J. Appl. Phys. (submitted), **(2004)**.

Interactions/Transitions

This patent has been licensed by Coatue Technology in Boston. It is a start-up company that will commercialize this memory device. Two years ago, Coatue was acquired by AMD.